2018

High temperature heat pump using HFO and HCFO refrigerants - System design, simulation, and first experimental results

Cordin Arpagaus
NTB University of Applied Sciences of Technology Buchs, Switzerland, cordin.arpagaus@ntb.ch

Frédéric Bless
NTB University of Applied Sciences of Technology Buchs, Institute for Energy Systems, Werdenbergstrasse 4, 9471 Buchs, Switzerland, frederic.bless@ntb.ch

Michael Uhlmann
NTB University of Applied Sciences in Buchs, Switzerland, michael.uhlmann@ntb.ch

Elias Büchel
NTB University of Applied Sciences of Technology Buchs, Institute for Energy Systems, Werdenbergstrasse 4, 9471 Buchs, Switzerland, elias.buechel@ntb.ch

Stefan Frei
NTB University of Applied Sciences of Technology Buchs, Institute for Energy Systems, Werdenbergstrasse 4, 9471 Buchs, Switzerland, stefan.frei@ntb.ch

See next page for additional authors

Authors
Cordin Arpagaus, Frédéric Bless, Michael Uhlmann, Elias Büchel, Stefan Frei, Jürg Schiffmann, and Stefan Bertsch

High temperature heat pump using HFO and HCFO refrigerants – System design, simulation, and first experimental results

Cordin ARPAGAUS[1]*, Frédéric BLESS[1], Michael UHLMANN[1], Elias BÜCHEL[1], Stefan FREI[1], Jürg SCHIFFMANN[2], Stefan S. BERTSCH[1]

[1]NTB University of Applied Sciences of Technology Buchs, Institute for Energy Systems, Werdenbergstrasse 4, 9471 Buchs, Switzerland

[2]Ecole Polytechnique Fédérale de Lausanne, Laboratory for Applied Mechanical Design, Rue de la Maladière 71b, 2002 Neuchâtel, Switzerland

* Corresponding Author: cordin.arpagaus@ntb.ch, +41 81 755 34 94

ABSTRACT

High temperature heat pumps (HTHPs) with heat sink temperatures in the range of 100 to 160°C are expected to become increasingly commercialized in the coming years. Major applications have been identified, particularly in the food, paper, metal and chemical industries, especially in drying, sterilization, evaporation, and steam generation processes. With the intensification of the F-gas regulations, only refrigerants with low GWP may be used in the near future. Replacement fluids for the currently applied hydrofluorocarbons (HFCs) R245fa and R365mfc are required.
The actual research gap in the field of HTHPs is to extend the limits of efficiency and heat sink temperature to higher values, while using environmentally friendly refrigerants. Natural refrigerants such as water (R718) or hydrocarbons (e.g. R601 or R600) are promising candidates. However, special heat pump cycle designs with multi-stage recompression or sophisticated safety measures against flammability are needed, which can increase system costs. Various hydrofluoroolefins (HFOs) and hydrochlorofluoroolefins (HCFOs) have recently been developed, which exhibit very low GWPs, are non-flammable and show potential for use at high temperatures (i.e. their critical temperatures are above 150°C). The thermodynamic properties of these fluids allow subcritical heat pump operation at condensation temperatures in the range of about 100 to 160°C.
This paper investigates the environmentally friendly HFOs R1336mzz(Z) and R1234ze(Z) and the HCFOs R1233zd(E) and R1224yd(Z) and compares the coefficient of performance (COP) and the volumetric heating capacity (VHC) with the HFC refrigerants R365mfc and R245fa at different condensation temperatures and temperature lifts. Based on simulations and literature findings, a single-stage HTHP with internal heat exchanger (IHX) has been designed and built to test the performance of various refrigerants and high-viscosity oils. The established laboratory scale HTHP provides 10 kW heating capacity and heat sink temperatures of 80 to 150°C. The system operates with a variable-speed reciprocating compressor and has an oil separator installed on the discharge side of the compressor. The IHX is used to ensure adequate superheating control. The system design, theoretical simulations and first experimental test results with R1233zd(E) are presented.

Keywords: high temperature heat pump, HFO, HCFO, refrigerant, low GWP, efficiency, COP

1. INTRODUCTION

High temperature heat pumps (HTHPs) with heat sink temperatures in the range of 100 to 150°C are suitable systems for waste heat recovery in various industrial processes, such as drying, sterilization, steam generation, papermaking, or food preparation (Arpagaus *et al.*, 2018). Low-temperature waste heat can be upgraded efficiently into usable high-temperature heat. Moreover, multi-temperature heat pump systems are suitable to make use of multiple waste heat sources and sinks at different temperature levels in order to further increase system efficiency (Arpagaus *et al.*, 2016).
In the area of HTHP technology development there is high research activity. Various experimental R&D projects are currently running on an international level to push HTHPs from the laboratory scale towards industry (Arpagaus *et al.*, 2018). The main research goals are extending the limits of heat sink temperatures to higher values, improving heat

pump efficiency, and testing new environmentally friendly refrigerants. With the intensification of the F-gas regulations only refrigerants with a GWP smaller than 150 may be used in new heat pumps for commercial use by 2022. The HFC refrigerants R245fa and R365mfc are subjected to phase down (i.e. production and consumption) in most developed countries. Natural refrigerants, such as water (R718) (Bertsch *et al.*, 2018; Chamoun *et al.*, 2014; De Larminat *et al.*, 2014), or hydrocarbons like R600 (Bamigbetan *et al.*, 2017; Moisi & Rieberer, 2017; Wemmers *et al.*, 2017) and R601 (Yamazaki & Kubo, 1985) are promising environmentally friendly replacement candidates. However, special heat pump cycle designs with multi-stage recompression or sophisticated safety measures against flammability are required, which can increase system costs.

In recent years, various HFOs and HCFOs have been developed with very low GWPs, non-flammability, and great potential for use at high temperatures. Heat sink temperatures of almost 160°C are reported by using the HFO R1336mzz(Z) (Fleckl *et al.*, 2015; Helminger *et al.*, 2016). Other studies report on fluids with no further published information on the chemical composition, such as LG6 (Reißner *et al.*, 2013) ÖKO1 (contains R245fa) (Wilk *et al.*, 2016), ECO3 (contains R245fa) (Bobelin *et al.*, 2012; Peureux *et al.*, 2012), HT125 (Noack, 2016), BY-4 (Yu *et al.*, 2014), or BY-5 (Zhang *et al.*, 2017). Most experimental studied cycles are single-stage. A few studies investigated two-stage cycles (Bamigbetan et al., 2017) or circuits with additional subcoolers for combined water heating (Bobelin *et al.*, 2012; Wemmers *et al.*, 2017). The experimentally achieved COPs in the laboratory systems range from about 5.7 to 6.5 at 30 K temperature lift and 2.2 to 2.8 at 70 K, respectively (Arpagaus *et al.*, 2018).

This paper investigates R1336mzz(Z), R1234ze(Z), R1233zd(E), and R1224yd(Z) in terms of their suitability for application in HTHPs. Theoretical simulations compare the COPs and VHCs with the HFC refrigerants R365mfc and R245fa at different condensation temperatures and temperature lifts of 30 and 70 K. Based on those findings, a single-stage laboratory scale HTHP system has been designed and built with a heating capacity of 10 kW and heat sink temperatures of 80 to 150°C. The theoretical simulations, the system design consideration, and the first experimental test results with the refrigerant R1233zd(E) are presented.

2. THEORETICAL SIMULATION

2.1 Refrigerants selection

Table 1 compares the properties of the low GWP HFO and HCFO refrigerants R1336mzz(Z), R1234ze(Z), R1233zd(E) and R1224yd(Z). The advantages of R1336mmz(Z) are the high critical temperature of 171.3°C at a feasible pressure of 29.0 bar. Its safety class is A1, and it has a GWP of 2, an ODP of 0, and an atmospheric life of only 22 days (Myhre *et al.*, 2013). Chemours is about to commercialize R1336mzz(Z) under the brand Opteon ™ MZ. It is stable up to 250°C for organic Rankine cycles, waste heat recovery applications, and steam generation (Kontomaris, 2014). Laboratory tests have shown that the material compatibility relative to copper and steel is similar to that of R245fa. Polyol ester oil (POE) with high viscosity is recommended as lubricant, as it is fully miscible over wide ranges of temperatures and compositions. Relatively little information is available on R1234ze(Z), which has a critical temperature of 150.1°C and a critical pressure of 35.3 bar (Kondou & Koyama, 2015). Its GWP is < 1 (Myhre *et al.*, 2013) and its flammability is rated with A2L (Fukuda *et al.*, 2014). R1234ze(Z) is assessed as a promising drop-in substitute for R114 in HTHP applications (Brown *et al.*, 2009).

R1233zd(E) with a critical temperature of 165.5°C and a critical pressure of 35.7 bar is available as Solstice®zd from Honeywell and is recommended for HTHP applications. Although R1233zd(E) contains chlorine, its ODP is extremely small (0.00034) due to the short atmospheric life of 40.4 days (Patten & Wuebbles, 2010).

Table 1. Properties of HFO and HCFO refrigerants suitable for HTHP application. ODP (UNEP, 2017), GWP_{100} (Myhre *et al.*, 2013), SG: Safety group classification (ASHRAE, 2016), NBP: Normal boiling point at 1.013 bar, M: molecular weight, Approximate sales price per kg refrigerant (based on a 10 kg container, prices from PanGas, Climalife, and Solvay, October 2017), n.a.: price not yet available but the refrigerant is close to market.

Type	Refrigerant	Chemical formula	T_{crit} [°C]	p_{crit} [bar]	ODP [-]	GWP_{100} [-]	SG	NBP [°C]	M [g/mol]	Price [EUR/kg]
HFO	R1336mzz(Z)[a]	$CF_3CH=CHCF_3(Z)$	171.3	29.0	0	2	A1	33.4	164.1	n.a.
	R1234ze(Z)[b]	$CF_3CH=CHF(Z)$	150.1	35.3	0	<1	A2L	9.8	114.0	n.a.
HCFO	R1233zd(E)[c]	$CF_3CH=CHCl(E)$	166.5	36.2	0.00034	1	A1	18.0	130.5	50
	R1224yd(Z)[d]	$CF_3CF=CHCl(Z)$	155.5	33.3	0.00012	<1	A1	14.0	148.5	n.a.
HFC (for comparison)	R365mfc[e]	$CF_3CH_2CF_2CH_3$	186.9	32.7	0	804	A2	40.2	148.1	80
	R245fa[f]	$CHF_2CH_2CF_3$	154.0	36.5	0	858	B1	14.9	134.0	57

[a]Opteon ™ MZ from Chemours, [b]Fukuda *et al.* (2014), [c]Solstice®zd from Honeywell (2016), [d]AMOLEA®1224yd from AGC Chemicals (2017), [e]Solkane®365mfc from Solvay, [f]Genetron® 245fa from Honeywell.

R1224yd(Z) is another A1 non-flammable HCFO refrigerant designed mainly for use in centrifugal chillers and waste heat recovery heat pumps. AGC Asahi Glass is going to market the refrigerant as Amolea®1224yd with commercial production beginning in early 2018 (AGC Chemicals, 2017). With an almost zero ODP (0.00012, atmospheric life of 21 days) and a GWP < 1, R1244yd(Z) has little impact on the environment. Its physical properties are close to R245fa and R1233zd(E). Furthermore, it has also good compatibility with most commonly used metals, plastics, and elastomers, and it is miscible with POE oils.
From a price perspective, R1233zd(E) costs about 50 EUR per kg, which is comparable to R245fa (57 EUR per kg) or R365mfc (80 EUR per kg). The prices of R1336mzz(Z) and R1224yd(Z) are not yet available but the refrigerants are close to market introduction.

2.2 Cycle selection

In order to compare the thermodynamic efficiency of the selected refrigerants, a simulation was performed for an idealized heat pump cycle with internal heat exchanger (IHX). Figure 1 illustrates the different thermodynamic states. This heat pump cycle offers a simple configuration and requires only a minimum number of equipment components. It is most favorable as a tradeoff between cycle complexity and efficiency (Moisi & Rieberer, 2017). A sufficiently high superheating is necessary to ensure a dry compression and to avoid cutting the saturation curve during compression, especially at high temperature lifts. An IHX is a simple concept for realizing the required superheating and simultaneously subcooling the liquid after condensation. The minimum superheat depends mainly on the refrigerant type, the condensation and evaporation temperatures, and the isentropic compressor efficiency. R1233zd(E) and R245fa require less than 10 K minimum superheat (Moisi & Rieberer, 2017), while R1336mzz(Z) requires at least 11 K superheat for a 40 K lift (based on isentropic compression $\eta_{is}=1$) (Kontomaris, 2013).

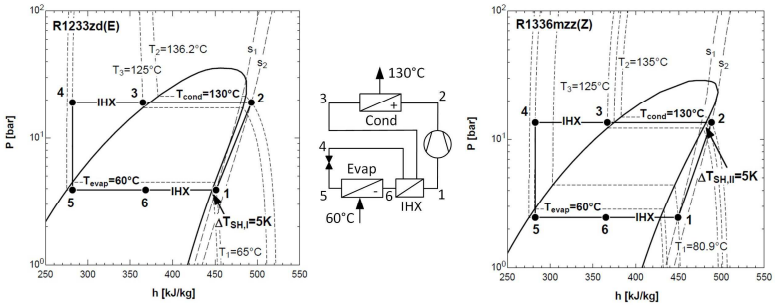

$$VHC = \rho_1(h_2 - h_3) \quad (1)$$

$$COP = (h_2 - h_3)/(h_2 - h_1) \quad (2)$$

Figure 1. Heat pump cycle with IHX and log(p)-h diagrams of R1233zd(E) ($\Delta T_{SH,I}$= 5 K at compressor inlet) and R1336mzz(Z) ($\Delta T_{SH,II}$ = 5 K at compressor outlet) at 60°C evaporation and 130°C condensation (70 K lift).

2.3 Assumptions

The simulation model was developed using the software EES (V10.268, Klein, 2017), assuming:

- A constant compressor isentropic efficiency of 0.7 (Bobelin *et al.*, 2012; Kontomaris, 2014)
- 5 K superheating ($\Delta T_{SH,I}$) at compressor inlet (suction) for R1233zd(E), R1234ze(Z), and *R245fa*
- 5 K superheating ($\Delta T_{SH,II}$) at compressor outlet (discharge) for *R365mfc*, R1336mzz(Z), and R1224yd(Z)
- 5 K subcooling (ΔT_{SC}) (i.e. low heat sink temperature glide as in drying and steam generation applications)
- 5 K minimum temperature difference within the IHX (ΔT_{IHX} between the state points 6 and 4)
- No pressure losses in any components but in the expansion valve (isenthalpic expansion, $h_5=h_4$)
- No heat losses in any components but heat exchangers (condenser, evaporator, IHX)

The COP and the VHC were calculated according to Eq. (1) and (2) for a condensation temperature range between 60 and 200°C at a fixed temperature lift of 70 and 30 K. The VHC was derived from the product of the enthalpy difference supplied to the heat sink ($h_2 - h_3$) and the suction vapor density (ρ_1). It describes the generated heat capacity per processed volume of refrigerant suction vapor and determines the compressor size and cost, and it influences the achievable experimental COP. The thermodynamic properties of the refrigerants were obtained from the EES fluid database, except for R1224yd(Z) which data was derived directly from literature (AGC Chemicals, 2017).

2.4 Simulation results

Figure 2 (a) shows the simulated COPs of the heat pump cycle with the different refrigerants as a function of the condensation temperature at a constant temperature lift of 30 and 70 K. The COPs exhibit an optimum, which is refrigerant dependent. The optimum occurs with condensation temperatures about 40 to 60 K below the critical

temperature. The optimum condensation temperatures for R1234ze(Z), R1224yd(Z), and R1233zd(E) are approx. 100 to 120°C, respectively. R365mfc provides the highest COP of all refrigerants at condensation temperature above 110°C with a maximum of about 3.2 (70 K lift) and 8.5 (30 K). R245fa exhibits the lowest COPs of all refrigerants. Above 80°C, the COPs of the HFO and HCFO refrigerants increase relative to R245fa, which is promising for HTHP applications in addition to the very low GWPs. The falling branches of the COP curves are associated with the narrowing of the two-phase region and the endpoint corresponds to the critical temperature of the respective fluid.
Figure 2 (b) compares the different VHCs for the selected refrigerants. The VHC curves increase with condensation temperature, which is equivalent to a higher evaporation pressure (at a fixed temperature lift), and thus higher suction vapor density (Kontomaris, 2015). Close to the critical point, the VHCs tend to flatten due to the decreasing latent heat in the condenser. A higher VHC is advantageous for positive displacement compressors (e.g. pistons and screws) as it requires a smaller swept volume at a given capacity, and thus smaller size and investment costs. For temperatures above 120°C, R1234ze(Z) offers the highest VHC among the investigated refrigerants. In comparison, R1224yd(Z), R245fa and R1233zd(E) appear promising with VHC values ranging from 2'500 to 3'400 kJ/m^3 at 130°C (and 70 K lift). The VHC values of R1336mzz(Z) are comparable to R365mfc and about 58% lower than R245fa resulting in a larger compressor. This is in agreement with other simulation studies where the decrease was about 65% (Kontomaris, 2014) and 41% (Kontomaris, 2014) at slightly different assumptions of superheating (20 K), subcooling (10 K), and isentropic compressor efficiency (0.8).

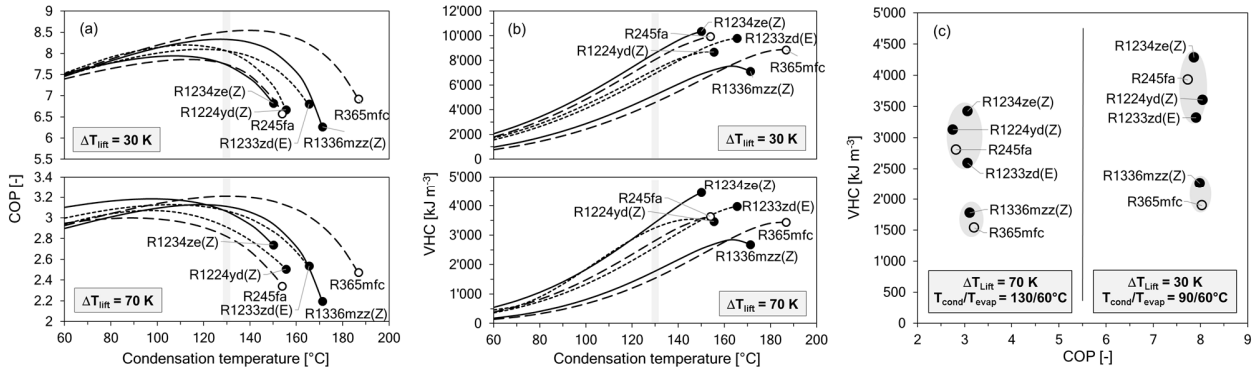

Figure 2. (a) Predicted COP and (b) VHC for the investigated refrigerants as a function of the condensation temperature at 30 and 70 K temperature lifts. (c) VHC versus COP at fixed temperature conditions.

Figure 2 (c) compares the calculated VHCs and COPs of the different refrigerants at fixed temperature conditions. The closest "drop-in" replacement for R365mfc would be R1336mzz(Z), whose COP and VHC are nearly identical (approx. 3% lower COP and 16% higher VHC). R1224yd(Z), R1234ze(Z) and R1233zd(E) are closer to R245fa, although their COPs are about 3% lower respectively 9% higher than the corresponding R245fa value.
Table 2 lists the simulated values including the discharge gas temperature (T_2), the pressure ratios (p_{ratio}), and the pressure levels at 60°C evaporation and 130°C condensation temperature. R1234ze(Z) exhibits the highest compressor discharge temperatures, which is critical in terms of compressor and oil stability. To mitigate the effects of the relatively high compressor discharge temperatures some equipment modifications (i.e. cooling means) would be required. The calculated pressure ratios of 4.8 to 5.8 are achievable with common positive displacement compressors. Overall, the cycle analysis suggests that there is a tradeoff between efficiency (high COP) and capacity (high VHC) when selecting a refrigerant for HTHP application.

Table 2. Simulation results of the heat pump cycle at fixed temperature conditions (ΔT_{Lift} = 30 and 70 K).

	ΔT_{Lift} = 30 K (T_{Evap}/T_{Cond} = 60°C/90°C)								**ΔT_{Lift} = 70 K (T_{Evap}/T_{Cond} = 60°C/130°C)**							
Refrigerant	**$\Delta T_{SH,I}$ [K]**	**$\Delta T_{SH,II}$ [K]**	**p_{Evap} [bar]**	**p_{Cond} [bar]**	**p_{ratio} [-]**	**T_2 [°C]**	**COP [-]**	**VHC [kJ/m^3]**	**$\Delta T_{SH,I}$ [K]**	**$\Delta T_{SH,II}$ [K]**	**p_{Evap} [bar]**	**p_{Cond} [bar]**	**p_{ratio} [-]**	**T_2 [°C]**	**COP [-]**	**VHC [kJ/m^3]**
R1233zd(E)	5	6.3	3.9	8.3	2.1	96.3	7.91	3'318	5	6.2	3.9	19.1	4.9	136.2	3.07	2'594
R1234ze(Z)	5	12.8	5.2	10.8	2.1	102.8	7.86	4'284	5	21.2	5.2	24.6	4.8	151.2	3.06	3'426
R245fa	*5*	*4.5*	*4.6*	*10.1*	*2.2*	*94.5*	*7.74*	*3'926*	*5*	*3.0*	*4.6*	*23.4*	*5.1*	*133.0*	*2.82*	*2'808*
R365mfc	*10.6*	*5*	*2.0*	*4.6*	*2.3*	*95*	*8.03*	*1'897*	*21.1*	*5*	*2.0*	*11.4*	*5.8*	*135*	*3.21*	*1'536*
R1336mzz(Z)	10.7	5	2.4	5.6	2.3	95	7.99	2'268	20.9	5	2.4	13.5	5.5	135	3.11	1'779
R1224yd(Z)	6.7	5	4.4	9.3	2.1	95	8.05	3'602	6.4	5	4.4	21.1	4.8	135	2.91	3'247

3. SYSTEM DESIGN AND TEST PROCEDURE

3.1 Experimental setup

Figure 3 illustrates the laboratory scale HTHP setup and its schematic diagram. Table 3 lists the main components of the HTHP system, the hydraulic loops, and the sensors with their measurement uncertainties. All components used are commercially available standard components without modifications.

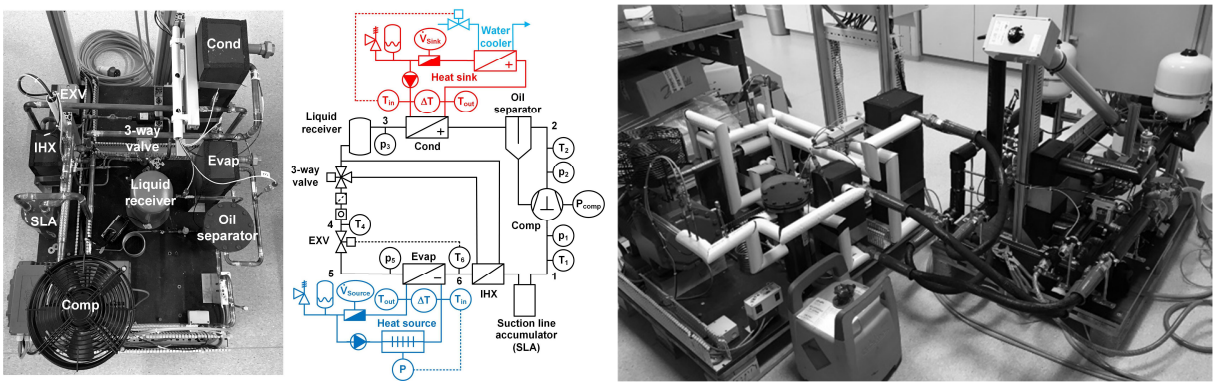

Figure 3. Experimental set-up and schematics of the HTHP (Right: Insulated with heat source and sink circuits).

Table 3. Components and instrumentation of the HTHP pilot plant.

	Component	Model type	Manufacturer	Description (max. allowed pressure, temperature), measuring range and accuracy
High temperature heat pump	Compressor	2DES-3Y New Ecoline	Bitzer	13.4 m^3/h at 50 Hz (1'450 rpm), POE oil: Reniso Triton SE 170
	Frequency converter	Vacon 100	Vacon	30 to 60 Hz setting (870 to 1'740 rpm)
	Condenser	B8LASHx30/1P-SC-M	SWEP	Plate heat exchanger, 0.708 m^2
	Evaporator	B25THx30/1P-SC-S	SWEP	Plate heat exchanger, 1.76 m^2
	Internal Heat Exchanger (IHX)	B5THx16/1P-SC-M	SWEP	Plate heat exchanger, 0.168 m^2
	Oil separator	Coalecent 922M	Temprite	Oil volume 0.4 L (max. 160°C, 45 bar)
	Dryer filter	Multiplex 083	Hansa	Molecular sieve 3Å and aluminum oxide (max. 120°C, 60 bar)
	Sight glass	SGP 10S N	Danfoss	With dry/moisture indicator (max. 80°C, 52 bar)
	Liquid receiver	FS56	Bitzer	Volume 5.6 L (max. 120°C, 33 bar)
	Suction line accumulator (SLA)	FA-22	ESK Schultze	Volume 3.5 L (max. 100°C, 28 bar)
	Expansion valve (EXV)	MVL661.15-0.4	Siemens	K_{VS} = 0.4 m^3/h, magnetic actuator (max. 140°C, 45 bar)
	3-way valve	M3FK15LX15	Siemens	K_{VS} = 1.5 m^3/h, magnetic actuator (max. 120°C, 32 bar)
	Safety pressure switch	KP17WB	Danfoss	32 bar (high pressure) and 0.7 bar (low pressure) settings
Hydraulic loops (heat source & sink)	Electrical heater	12R104-01	Backer ELC	Pipe model, heating capacity 10 kW (max. 110°C)
	Water pumps	HT-AY-2251-PM.0005	Speck Pumpen	Turbine pumps, 1'000 to 4'000 rpm (max. 40 L/min, 180°C)
	Frequency converters	Vacon 20	Vacon	30 to 60 Hz setting
	Rotary valves	NEBM24.2-05	Nenutec	2-way ball valves, actuator modulating (max. 80°C)
	Water cooler	WP4.24 (GBS400H-24)	GEA WTT/Kelvion	Plate heat exchanger, 0.77 m^2 (max. 31 bar)
	Expansion tanks	VS8	Solardirekt24	Volume 8 L, with EPDM membrane (max. 140°C, 10 bar)
	Safety relief valves	Solar 253	Caleffi Solar	Diaphragm safety valves (max. 160°C, 6 bar)
	Pressure gauges	232.50	WIKA	(max. 200°C, 10 bar)
	Bleed air vents	SV50	Solardirekt24	(max. 180°C, 10 bar)
Sensors	Pressure sensors	PAA-21Y (piezoelectric)	Keller	0 to 5, 10, and 50 bar (max. 120°C), max. 1.5% of full scale
	Thermocouples	Type K (class 1)	Alphasol Tec	-25 to +400°C, ± 1.5 K (absolute), ± 0.1 K (differential)
	Power transmitter	ITL-101	Infratek	0 to 15 kW range, 0.2% of measuring range + 0.1% of reading
	Volume flow transmitter	SBT633 (mechatronic)	IFM Electronic	0.3 to 25 L/min (max. 180°C), 5% accuracy, 1% repeatability

The experimental setup consists of the actual HTHP system and two hydraulic loops for the heat source and heat sink. The heat source circuit simulates potentially available waste heat of 40 to 80°C from an industrial process and includes a controllable electrical heater, a water pump with adjustable volume flow, a diaphragm expansion tank, a safety valve and a vent valve. The heat sink simulates the HTHP application (e.g. potential steam generation or a drying process) and comprises a tap water cooler to release the produced heat to the environment. Pressurized water of 3 to 5 bar is used in both hydraulic circuits to prevent steam generation inside the loops. The water pumps are regenerative turbine pumps with magnet permanent synchronous motors (stable up to 180°C). Temperature resistant steam hoses (Goodall® Inferno models) connect the HTHP inlets and outlets to both hydraulic loops.

The actual HTHP consists of a simple heat pump cycle with an internal heat exchanger (IHX). The IHX transfers heat from the liquid refrigerant after the condenser outlet to the suction gas and thereby increases the suction gas temperature (T_1) and ensures adequate superheating control. The refrigerant mass flow through the IHX can be continuously adjusted via a 3-way valve (with magnetic actuator and approx. 1 sec positioning time). A setting of 0% IHX corresponds to the operation of a simple heat pump cycle, while 100% fully incorporates the IHX into the cycle. A variable-speed semi-hermetic piston compressor drives the HTHP. An external frequency converter adjusts the compressor speed within the allowed limits (30 to 60 Hz corresponds to 870 to 1'750 rpm). An integrated PTC sensor prevents overheating of the motor windings. The switch-off temperature is at approx. 100°C. The ventilator of the compressor was turned off during the experiments. R1233zd(E) is used as a refrigerant (Solstice®zd from Honeywell), as it is non-toxic, non-flammable, environmentally safe, and offers a high critical temperature of 166.5°C. Its physical properties and theoretical performance are comparable to R245fa (see section 2). The refrigerant has been charged as gas at the reference point operating conditions (W60/W110), whereby the presence of the liquid state in the sight glass was checked. The filling charge is 4.2 kg. A coalescent oil separator is installed on the discharge side, which traps the oil and redirects it back to the compressor through an oil cooling tube. A POE oil with a viscosity of 170 mm^2/s (at 40°C) is used to achieve a sufficient lubrication at the high operating temperatures. A liquid receiver acts as refrigerant storage vessel. The condenser, evaporator and IHX are compact plate heat exchangers developed with low-pressure drop. The evaporator generates vapor from the externally supplied hot water at 60 to 80°C. The condenser transfers the generated heat (range of 70 to 150°C) to the heat sink loop. A suction line accumulator (SLA) prevents direct liquid entry into the compressor if the evaporator and IHXs are unable to superheat the fluid sufficiently. Temperature resistant Armaflex HT (max. 150°C) insulation is used to insulate the copper tubing. Not insulated are the oil separator, the liquid receiver, and the SLA. A series of temperature, pressure, flow rate, and power sensors are installed at several locations of the experimental system. The temperatures are measured by thermocouples (type K, class 1), which have been calibrated in a silicone oil bath from 20 to 110°C with an accuracy of ± 0.1 K. Thermocouples with differential temperature measurement (ΔT) are installed at the inlets and outlets of the hydraulic loops (heat source and sink). The flow sensors in the respective hydraulic loops have been calibrated at 60°C with a certified Coriolis sensor (Promass 83E from E+H). The repeatability in the operating range of the test conditions is ± 1%. A power analyzer measures the electrical power consumption of the compressor with an accuracy of ± 3 %. A CompactRIO Platform from National Instruments (cRIO-9022 with 8 slots) in combination with LabVIEW™2017myRio is used for data acquisition and controlling the experimental set-up with a sampling time of 1 second.

3.2 Test procedure and process parameters

After heating up the HTHP system to a specific measurement point (see the experimental runs and process parameters in Table 4) and reaching steady state conditions, the HTHP was operated in steady state conditions for several minutes per run. Mean values were calculated and used for data analysis. The heat source inlet temperature was varied between 40, 60 and 80°C and the heat sink outlet temperature between 70, 90, 110, 130, and 150°C. The electrical heater controlled the heat source inlet temperature (T_{in}) and the rotary valve at the water cooler inlet the heat sink inlet temperature (both by PI controls in LabVIEW). After reaching the desired heat source and heat sink temperatures, the speed of the water pumps were adjusted manually to fit a heat source temperature difference of 3.0 ± 0.1 K and a heat sink temperature spread of 5.0 ± 0.1 K, which is in accordance with the standard DIN EN 14511. The expansion valve controlled the superheating after the evaporator (PI control). A superheating of 5 K was set for all experiments. The suction gas superheating (ΔT_{SH}) and the liquid subcooling (ΔT_{SC}) were calculated using Eq. (3) and (4). The heating COP of the HTHP and the Second Law efficiency (η_{2nd}) was determined by Eq. (5) and (6):

$$\Delta T_{SC} = T(p_3) - T_4 \quad (3)$$

$$\Delta T_{SH} = T(p_5) - T_6 \quad (4)$$

$$COP = \dot{Q}_{Sink}/P_{comp} = \left(c_p(T) \cdot \rho(T) \cdot \dot{V}_{Sink} \cdot \Delta T_{Sink}\right)/P_{comp} \quad (5)$$

$$\eta_{2nd} = COP/COP_{Carnot} \text{ with } COP_{Carnot} = T_{Sink,out}/\left(T_{Sink,out} - T_{Source,in}\right) \quad (6)$$

where $\dot{V}_{Sink}$ corresponds to the water flow rate and ΔT_{Sink} is the temperature difference between outlet and inlet of the heat sink. The properties of water ($c_p(T)$ and $\rho(T)$) were fitted according to data listed in the VDI-Wärmeatlas (VDI, 2006). The electrical power consumed by the compressor (P_{comp}) was used to calculate the COP. The electrical power consumed by the water pumps (0.25 to 1.75 kW each) and for controlling the heat pump unit (about 110 W) was not considered in the COP calculation. A parameter study examined the influence of the temperature lift (30, 50 and 70 K), the compressor speed (30 to 60 Hz: 870 to 1'750 rpm), the temperature glide on the heat sink (5, 20, and 30 K), and the setting of the IHX (0 to 100%) on the Second Law efficiency (η_{2nd}) and COP.

4. EXPERIMENTAL TEST RESULTS AND DISCUSSION

Table 4 shows the examined process parameters and the results of the parameter study. The Figures 4 (a) to (f) illustrate the main findings graphically. Figure 4 (a) shows the performance map of the HTHP as a function of the investigated heat source and heat sink temperatures at 30, 50 and 70 K temperature lift. The COP increases with a smaller temperature lift ($T_{Sink,out} - T_{Source,in}$) and higher heat sink outlet temperature ($T_{Sink,out}$) according to Carnot's relation (Eq. 6). At the reference point (Run 5 Ref, W60/W110, 50 K lift) a COP of 2.43 was reached with a reproducibility of 3.1% (ΔCOP = ± 0.08, standard deviation derived from 8 runs at different operating dates). The calculated measurement uncertainty of the COP was between 4 to 7 %. The maximum delivered heat sink temperature was 151°C from a heat source at 80°C (at a lift of 71 K, Run 9). In average, the discharge temperature (T_2) was approx. 5 K above the heat sink outlet temperature.

Figure 4 (b) illustrates the same experimental COP data as a function of the $T_{Sink,out}$ and the respective ΔT_{Lift}. The decreasing COP curve at 70 K lift is attributed to (1) the narrower two-phase region for condensation closer to the critical temperature, as well as to (2) increasing heat losses ($\dot{Q}_{Loss}$) of the system due to natural convection and radiation at elevated temperatures, since the system is not insulated well yet. From the energy balance over the heat pump ($\dot{Q}_{Loss} \approx \dot{Q}_{Source} + P_{Comp} - \dot{Q}_{Sink}$) heat losses between 15% (at 70°C) and 45% (at 150°C) are estimated, leading to rather low Second Law efficiencies of 19 to 32%. For comparison, Fleckl *et al.* (2015) reported η_{2nd} values of 35 to 50%. Thus, there is considerable potential for optimization in insulation and room for efficiency improvement. Figure 4 (b) also shows the COP of the tests at ΔT_{Lift} = 50 K with 100% IHX (Runs 21, 22, and 23). The IHX leads to a COP increase of about 14% compared to the basic heat pump cycle. This is in agreement with experimental studies of Helminger *et al.* (2016), where an efficiency increase of 4 to 10% and 19 to 47% was reported at 35 K and 60 K temperature lift using an IHX and R1336mzz(Z).

Figure 4 (c) shows the heating capacity ($\dot{Q}_{Sink}$) as a function of the heat source inlet temperature ($T_{Source,in}$). The heating capacity increases steadily with temperature at a given temperature lift (see Carnot's relation Eq. 6). At the reference point conditions (Run 5 Ref), the heating capacity is about 5.1 kW. At W80/W111 (Run 7) a heating capacity of close to 10 kW could be measured. At this point, the HTHP setup reaches its experimental capacity limits.

The graphs (d), (e) and (f) in Figure 4 show the influence of the compressor frequency, the heat sink temperature glide, and the IHX on the COP. Each process parameter was varied from the reference point condition (Ref), while the other parameters were kept constant. The compressor power and the heating capacity of the HTHP increased almost linearly with compressor frequency (speed). At about 50 Hz an optimal COP of the heat pump was reached. At lower frequency, the COP of the heat pump reduced indicating a less efficient operating region of the compressor.

Table 4: Process and performance parameters of the experimental test runs (Run 5 Ref: Reference point conditions).

No.	$T_{Source,in}$ °C	$T_{Sink,out}$ °C	ΔT_{Lift} K	ΔT_{Source} K	ΔT_{Sink} K	T_1 °C	T_2 °C	ΔT_{SH} K	ΔT_{SC} K	*IHX* %	f Hz	p_{Cond} bar	p_{Evap} bar	p_{ratio} -	P_{Comp} kW	$\dot{Q}_{Sink}$ kW	$\dot{Q}_{Source}$ kW	$\dot{Q}_{Loss}$ kW	η_{2nd} %	*COP* -
1	40	71	**31**	3.0	5.1	38	81	5.0	5.0	0	50	5.3	1.8	3.3	1.2	4.3	3.9	0.8	32%	3.6
2	40	90	**50**	3.0	5.1	39	93	5.0	6.7	0	50	8.6	1.8	5.2	1.4	3.2	3.0	1.2	31%	2.3
3	40	109	**69**	3.1	5.1	40	110	5.0	8.6	0	50	12.8	1.8	7.6	1.5	2.3	2.1	1.3	27%	1.5
4	60	91	**31**	3.2	5.0	57	97	5.0	4.6	0	50	8.8	3.3	3.0	1.7	6.6	7.7	2.8	32%	3.8
5 Ref	**60**	**110**	**50**	**3.0**	**5.0**	58	115	5.0	5.7	**0**	**50**	13.4	3.3	4.5	2.1	5.1	4.8	1.8	32%	2.4
6	60	130	**70**	3.0	4.7	58	132	5.0	7.9	0	50	19.6	3.3	6.4	2.3	3.2	3.1	2.3	24%	1.4
7	80	111	**31**	4.4	5.0	76	118	5.0	4.7	0	50	13.6	5.3	2.9	2.5	9.9	10.5	3.0	32%	4.0
8	80	130	**50**	3.2	5.0	77	135	5.0	5.3	0	50	19.8	5.6	3.9	3.1	7.2	7.7	3.6	29%	2.3
9	80	151	**71**	3.2	5.1	78	156	5.0	5.8	0	50	28.8	5.7	5.4	3.5	4.0	3.7	3.3	19%	1.1
10	60	111	51	3.0	**21.6**	58	114	5.0	5.9	0	50	13.4	3.3	4.4	2.1	5.8	4.8	1.1	37%	2.8
11	60	109	49	3.2	**29.8**	58	112	5.0	6.7	0	50	12.7	3.3	4.3	2.0	6.0	5.2	1.2	38%	2.9
12	60	110	50	2.9	5.0	57	111	5.0	6.7	0	**30**	13.1	3.3	4.1	1.3	2.5	2.7	1.5	26%	2.0
13	60	110	50	3.0	5.1	58	111	5.0	6.7	0	**35**	13.2	3.3	4.2	1.4	3.1	3.1	1.5	28%	2.1
14	60	110	50	3.0	5.0	58	112	5.0	6.2	0	**40**	13.3	3.3	4.3	1.6	3.7	3.5	1.5	29%	2.2
15	60	110	50	3.1	5.0	58	117	5.0	5.2	0	**60**	13.4	3.3	4.6	2.5	6.0	5.8	2.2	31%	2.4
16	60	111	51	3.0	5.0	58	119	5.0	7.4	**7.5**	50	13.5	3.3	4.5	2.1	5.3	4.9	1.7	34%	2.6
17	60	110	50	3.0	4.9	85	131	5.0	25.7	**20**	50	13.4	3.3	4.5	2.1	5.6	6.2	2.7	35%	2.7
18	60	110	50	3.0	5.1	87	134	5.0	27.3	**30**	50	13.3	3.3	4.4	2.1	5.7	6.4	2.8	36%	2.7
19	60	110	50	3.0	5.1	90	137	5.0	29.4	**50**	50	13.3	3.3	4.5	2.1	5.8	6.7	3.0	36%	2.7
20	60	110	50	3.0	5.2	90	137	5.0	29.3	**75**	50	13.3	3.3	4.5	2.1	5.9	6.6	2.8	36%	2.8
21	60	110	**50**	3.1	5.0	90	137	5.0	29.2	**100**	50	13.4	3.3	4.4	2.1	5.9	6.8	3.0	36%	2.8
22	40	90	**50**	3.0	5.0	71	114	5.0	29.4	**100**	50	8.5	1.8	5.2	1.4	3.6	3.5	1.3	36%	2.6
23	80	131	**51**	4.2	5.2	110	157	5.0	28.5	**100**	50	20.1	5.5	4.0	3.2	8.4	10.0	4.7	34%	2.7

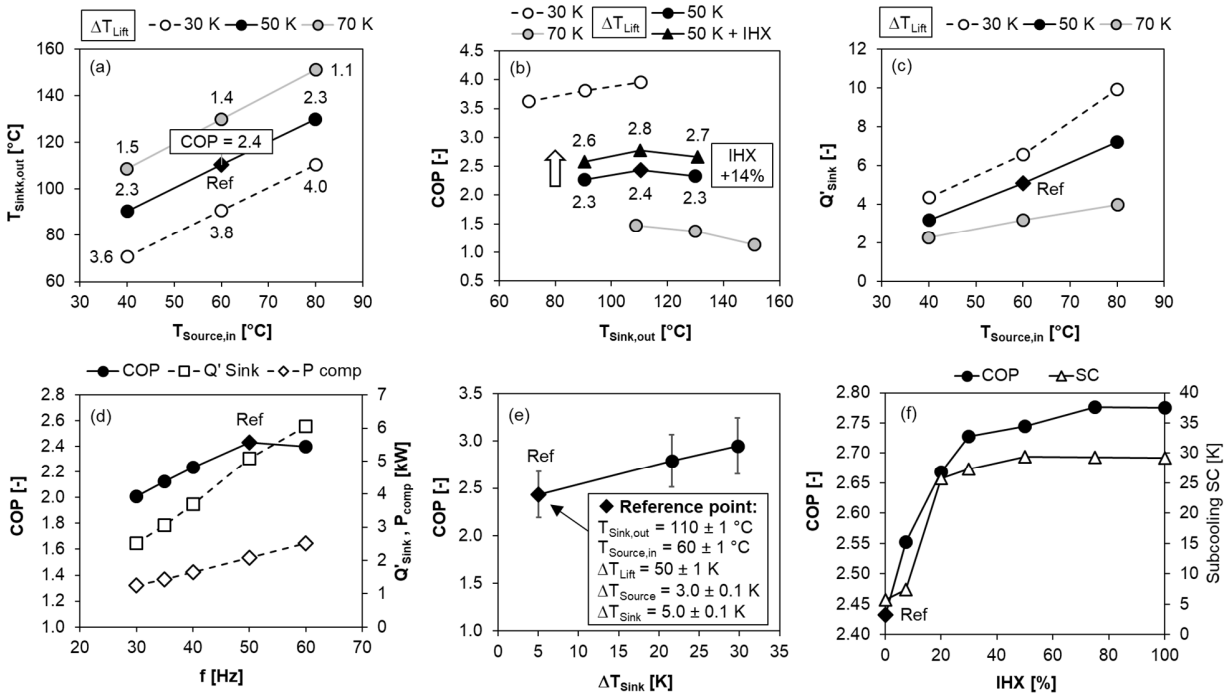

Figure 4. Experimental performance data of the studied HTHP. (a) Operating map, (b) Temperature lifts, (c) Heating capacity, (d) COP vs. compressor speed, (e) COP vs. heat sink temperature glide, and (f) COP vs. IHX.

Figure 4 (e) presents the effect of a higher heat sink temperature difference (ΔT_{Sink}) on the COP (Runs 5, 10 and 11). As the temperature glide rises (from 5 to 30 K), the subcooling increases (from 5.7 to 6.7 K) and the efficiency of heat exchange in the condenser improves, which leads to a 19% higher heating capacity and 21% higher COP.
Figure 4 (f) shows the influence of the IHX on the COP from 0 to 100% setting of the 3-way valve. The expansion valve is controlled by the superheat at the evaporator outlet (not IHX outlet), which means that the superheating area in the evaporator remains constant. Compared to the basic heat pump cycle (0% IHX setting, Ref), the suction gas is additionally superheated in the IHX. As the mass flow rate through the IHX increases, the COP as well as the compressor suction (T_1) and discharge temperatures (T_2) increase. The COP levels off with increasing IHX flow, indicating a sufficiently large IHX heat exchanger. During operation, the regulation with the 3-way-valve and the addition of the IHX ensures flexibility in superheating control, which is promising for future applications using alternative low GWP refrigerants exhibiting high superheating requirements (Reißner *et al.*, 2013). Too high discharge gas temperatures are confined by the switch-off temperature of the compressor. For the operating point W80/W131 (Run 23) the suction (T_1) and discharge temperatures (T_2) were 110°C and 157°C respectively and thus close to the set compressor limit.

After the presented first experimental test results with the newly developed HTHP and the refrigerant R1233zd(E), an experimental review revealed the following optimization potentials for further studies:

- Improvement of the insulation of the HTHP system to reduce the heat losses at elevated temperatures. A significant increase in efficiency is expected as the COP increases proportionally with lower heat losses.
- Reduction of the actual measurement uncertainties by implementation of more precise temperature measurement with calibrated PT100 sensors and a temperature-resistant Corriolis flow meter on the heat sink side.
- Performing further tests with alternative refrigerants with low GWP (see section 2) which also allow heat sink temperatures above 150°C. For comparison, Helminger *et al.* (2016) reported heat sink temperatures of almost 160°C with the HFO refrigerant R1336mzz(Z). COP values of 2.7 were achieved with a temperature lift of 45 K (heat source to sink temperatures). Fleckl *et al.* (2015) reached 150°C with a COP of 2.4 and a significant temperature lift of 70 K (evaporation to condensation temperature).

5. CONCLUSIONS

Theoretical simulations of a basic heat pump cycle with various low GWP HFO and HFCO refrigerants revealed a tradeoff between performance (COP) and volumetric heating capacity (VHC). R1336mzz(Z) was found to be the next drop-in replacement for R365mfc. The performance figures of R1224yd(Z), R1234ze(Z) and R1233zd(E) were closer to R245fa. Based on those findings, a laboratory scale high temperature heat pump (HTHP) was designed, built and tested with the commercially available HFCO refrigerant R1233zd(E). Standard components were used to construct the experimental test setup. The developed HTHP is single-stage, operates with a piston compressor and contains a continuously adjustable internal heat exchanger (IHX) for superheating and efficiency increase. The use of the IHX increased the heating COP significantly (+14%) compared to a simple heat pump cycle. The heat pump circuit is relatively easy to control. The basic functionality of the developed HTHP system for potential industrial process applications (e.g. drying processes or steam generation) could be demonstrated by operating the heat pump at heat source temperatures of 40 and 80°C and heat sink temperatures between 70 and 150°C. At the reference point condition (W60/W110, 50 K temperature lift) a COP of 2.43 was reached. The performance data of the HTHP could be examined at 30, 50 and 70 K temperature lifts over the entire operating map. In particular, a COP increase of 21% was achieved by increasing the heat sink temperature difference from 5 to 30 K. The results are promising as the developed HTHP system allows testing alternative HFO and HCFO refrigerants like R1336mzz(Z) and R1224yd(Z) in the future. Further efficiency improvements can be achieved through the reduction of thermal losses at elevated temperatures by better insulation of the heat pump components and tubing. A further increase in the heating COP can be expected.

NOMENCLATURE

COP	coefficient of performance (–)
c_p	specific heat capacity (kJ/kg-K)
ρ	density (kg/m^3)
ΔT	temperature difference (K)
GWP	global warming potential, 100 years
h	enthalpy (kJ/kg)
HCFO	hydrochlorofluoroolefin
HFC	hydrofluorocarbon
HFO	hydrofluoroolefin
HTHP	high temperature heat pump
IHX	internal heat exchanger
ODP	ozone depletion potenial
p	pressure (bar)
P	electrical power (kW)
POE	polyolester oil
$\dot{Q}$	heating capacity (kW)
Ref	reference point conditions
SG	safety group classification
T	temperature (°C)
VHC	volumetric heating capacity (kJ/m^3)
$\dot{V}$	volume flow (m^3/s)

Subscripts

Comp	compressor
Cond	condensation, condenser
crit	critical temperature
Evap	evaporation, evaporator
IHX	internal heat exchanger
in	inlet
Lift	temperature lift
out	outlet
Sink	heat sink
Source	heat source
1 … 6	state points numbering

REFERENCES

AGC Chemicals. (2017). AMOLEA® 1224yd, Technical Information, ASAHI Glass Co., Ltd.

Arpagaus, C., Bless, F., Schiffmann, J., & Bertsch, S. S. (2016). Multi-temperature heat pumps: A literature review. *International Journal of Refrigeration*, *69*, 437–465. https://doi.org/10.1016/j.ijrefrig.2016.05.014

Arpagaus, C., Bless, F., Uhlmann, M., Schiffmann, J., & Bertsch, S. S. (2018). High temperature heat pumps: Market overview, state of the art, research status, refrigerants, and application potentials. *Energy*, *152*, 985–1010. https://doi.org/http://dx.doi.org/10.1016/j.energy.2018.03.166

ASHRAE. (2016). Standard 34 - Safety Standard for Refrigeration Systems and Designation and Classification of Refrigerants.

Bamigbetan, O., Eikevik, T. M., Nekså, P., & Bantle, M. (2017). Development of propane-butane cascade high temperature heat pump: Early test rig results. In *International Workshop on High Temperature Heat Pumps, Sept 9, 2017, Copenhagen, Denmark* (pp. 1–12). Retrieved from http://www.sintef.no/heatup

Bertsch, S., Arpagaus, C., Bless, F., Weickgenannt, A., & Schiffmann, J. (2018). Theoretical Investigation of a High Temperature Heat Pump using a Micro Turbo Compressor and Water as a Refrigerant, Paper ID 201. In *13th IIR-Gustav Lorentzen Conference on Natural Refrigerants, 18-20 June 2018, Valencia, Spain* (pp. 1–9).

Bobelin, D., Bourig, A., & Peureux, J. (2012). Experimental results of a newly developed very high temperature industrial heat pump (140°C) equipped with scroll compressors and working with a new blend refrigerant, Paper 1299. In *International Refrigeration*

and Air Conditioning Conference (pp. 1–10). Retrieved from http://docs.lib.purdue.edu/iracc/1299

Brown, J. S., Zilio, C., & Cavallini, A. (2009). The fluorinated olefin R-1234ze(Z) as a high-temperature heat pumping refrigerant. *International Journal of Refrigeration*, *32*(6), 1412–1422. https://doi.org/10.1016/j.ijrefrig.2009.03.002

Chamoun, M., Rulliere, R., Haberschill, P., & Peureux, J.-L. (2014). Experimental and numerical investigations of a new high temperature heat pump for industrial heat recovery using water as refrigerant. *International Journal of Refrigeration*, *44*, 177–188. https://doi.org/10.1016/j.ijrefrig.2014.04.019

De Larminat, P., Arnou, D., La Sausse, P., Clunet, F., & Peureux, J.-L. (2014). A high temperature heat pump using water vapor as working fluid. In *11th IIR Gustav Lorentzen Conference on Natural Refrigerants, GL 2014, China, 31 August - 2 September 2014*. https://doi.org/10.1046/j.1365-2222.2000.00820.x

Fleckl, T., Hartl, M., Helminger, F., Kontomaris, K., & Pfaffl. (2015). Performance testing of a lab-scale high temperature heat pump with HFO-1336mzz-Z as the working fluid. In *European Heat Pump Summit 2015, October 20-21, Nuremberg, Germany* (pp. 1–25).

Fukuda, S., Kondou, C., Takata, N., & Koyama, S. (2014). Low GWP refrigerants R1234ze(E) and R1234ze(Z) for high temperature heat pumps. *International Journal of Refrigeration*, *40*, 161–173. https://doi.org/10.1016/j.ijrefrig.2013.10.014

Helminger, F., Hartl, M., Fleckl, T., Kontomaris, K., & Pfaffl, J. (2016). Hochtemperatur Wärmepumpen Messergebnisse einer Laboranlage mit HFO-1336MZZ-Z bis 160°C Kondensationstemperatur. In *14. Symposium Energieinnovation, 10.-12. Februar 2016, TU Graz* (pp. 1–20). Retrieved from www.tugraz.at/events/eninnov2016

Honeywell. (2016). Solstice refrigerants roadmap: The future of refrigerants, Brochure FPR-004-2016-09-EN.

Klein, S. A. (2017). Engineering Equation Solver (Version V10.268): F-Chart Software. Retrieved from www.fChart.com

Kondou, C., & Koyama, S. (2015). Thermodynamic assessment of high-temperature heat pumps using low-GWP HFO refrigerants for heat recovery. *International Journal of Refrigeration*, *53*, 126–141. https://doi.org/10.1016/j.ijrefrig.2014.09.018

Kontomaris, K. (2013). Low GWP Working Fluid for High Temperature Heat Pumps: DR-2, Chemical Stability at High Temperatures. In *European Heat Pump Summit 2013, October 15, 2013* (pp. 1–28). Retrieved from https://www.chemours.com/Refrigerants/en_US/products/Opteon/Stationary_Refrigeration/assets/downloads/2013_Charts-Chillventa.pdf

Kontomaris, K. (2014). A non-flammable, zero-ODP, low GWP working fluid for high temperature heat pumps: DR-148. In *11th IEA Heat Pump Conference, May 12-16, 2014, Montréal (Québec) Canada* (pp. 1–10).

Kontomaris, K. (2014). Zero-ODP, Low-GWP, Nonflammable Working Fluids for High Temperature Heat Pumps. In *ASHRAE Annual Conference, Seattle, Washington, July 1, 2014* (pp. 1–40).

Kontomaris, K. (2015). Zero-ODP, low GWP working fluids for high tempeature heating from low temperature heat: DR-14, DR-12 and DR-2. *Statewide Agricultural Land Use Baseline 2015*, *1*. https://doi.org/10.1017/CBO9781107415324.004

Moisi, H., & Rieberer, R. (2017). Refrigerant Selection and Cycle Development for a High Temperature Vapor Compression Heat Pump. In *12th IEA Heat Pump Conference 2017, Rotterdam2* (pp. 1–10).

Myhre, G., Shindell, D., Bréon, F.-M., Collins, W., Fuglestvedt, J., Huang, J., … Zhang, H. (2013). Anthropogenic and natural radiative forcing. In *Climate Change 2013: The Physical Science Basis. Contribution of Working Group I to the Fifth Assessment Report of the Intergovernmental Panel on Climate Change* (pp. 659–740). Cambridge, United Kingdom and New York, NY, USA: Cambridge University Press.

Noack, R. (2016). Entwicklung einer Hochtemperatur-Wärmepumpe für Nutztemperaturen über 120°C. In *Deutsche Kälte- und Klimatagung 2016, Kassel, 16.-18. November 2016, Kurzfassungen*.

Patten, K. O., & Wuebbles, D. J. (2010). Atmospheric lifetimes and Ozone Depletion Potentials of trans-1-chloro-3,3,3-trifluoropropylene and trans-1,2-dichloroethylene in a three-dimensional model. *Atmospheric Chemistry and Physics*, *10*(22), 10867–10874. https://doi.org/10.5194/acp-10-10867-2010

Peureux, J., Sapora, E., & Bobelin, D. (2012). Very high-temperature heat pumps applied to energy efficiency in industry. In *ACHEMA 2012, Frankfurt am Main, June 21, 2012* (pp. 1–23).

Reißner, F., Gromoll, B., Schäfer, J., Danov, V., & Karl, J. (2013). Experimental performance evaluation of new safe and environmentally friendly working fluids for high temperature heat pumps. In *European Heat Pump Summit 2013, October 15-16, 2013* (pp. 1–20).

UNEP. (2017). Handbook for the Montreal Protocol on Substances that Deplete the Ozon Layer, Eleventh edition.

VDI. (2006). *VDI-Wärmeatlas, 10. Auflage, Stoffwerte von Wasser, Dba*. Berlin Heidelberg: Springer.

Wemmers, A. K., Haasteren, A. W. M. B. van, & Kremers, P. K. J. van der. (2017). Test results R600 pilot heat pump. In *12th IEA Heat pump conference, Rotterdam, May 14-17, 2017* (pp. 1–9).

Wilk, V., Hartl, M., Fleckl, T., Widhalm, E., Ramler, F., Adelberger, G., … Ochsner, K. (2016). Hochtemperatur-Wärmepumpe für Industrieanwendungen: Prüfstandmessungen und Systemsimulation, IV.18. In *Deutsche Kälte- und Klimatagung 2016, Kassel, 16.-18. November 2016, Kurzfassungen.*

Yamazaki, T., & Kubo, Y. (1985). Development of a High-Temperature Heat Pump. *IEA Heat Pump Centre Newsletter, Vol. 3, No. 4*, 18–21.

Yu, X., Zhang, Y., Deng, N., Chen, C., Ma, L., Lipin, D., & Zhang, Y. (2014). Experimental performance of high temperature heat pump with near-azeotropic refrigerant mixture. *Energy and Buildings*, *78*, 43–49. https://doi.org/10.1016/j.enbuild.2013.12.065

Zhang, Y., Zhang, Y., Yu, X., Guo, J., Deng, N., Dong, S., … Ma, X. (2017). Analysis of a high temperature heat pump using BY-5 as refrigerant. *Applied Thermal Engineering*, *127*, 1461–1468. https://doi.org/10.1016/j.applthermaleng.2017.08.072

ACKNOWLEDGEMENT

This research project is part of the Swiss Competence Center for Energy Research SCCER EIP of the Swiss Innovation Agency Innosuisse.